5-2002

Hybrid Tetramers of Porcine Liver Fructose-1,6-bisphosphatase Reveal Multiple Pathways of Allosteric Inhibition

Scott W. Nelson
Iowa State University, swn@iastate.edu

Richard B. Honzatko
Iowa State University, honzatko@iastate.edu

Herbert J. Fromm
Iowa State University

Follow this and additional works at: http://lib.dr.iastate.edu/bbmb_ag_pubs

Part of the Biochemistry Commons, Chemistry Commons, and the Molecular Biology Commons

The complete bibliographic information for this item can be found at http://lib.dr.iastate.edu/bbmb_ag_pubs/74. For information on how to cite this item, please visit http://lib.dr.iastate.edu/howtocite.html.

Hybrid Tetramers of Porcine Liver Fructose-1,6-bisphosphatase Reveal Multiple Pathways of Allosteric Inhibition

Abstract

Fructose-1,6-bisphosphatase is a square planar tetramer of identical subunits, which exhibits cooperative allosteric inhibition of catalysis by AMP. Protocols for *in vitro* subunit exchange provide three of five possible hybrid tetramers of fructose-1,6-bisphosphatase in high purity. The two hybrid types with different subunits in the top and bottom halves of the tetramer co-purify. Hybrid tetramers, formed from subunits unable to bind AMP and subunits with wild-type properties, differ from the wild-type enzyme only in regard to their properties of AMP inhibition. Hybrid tetramers exhibit cooperative, potent, and complete (100%) AMP inhibition if at least one functional AMP binding site exists in the top and bottom halves of the tetramer. Furthermore, titrations of hybrid tetramers with AMP, monitored by a tryptophan reporter group, reveal cooperativity and fluorescence changes consistent with an R- to T-state transition, provided that again at least one functional AMP site exists in the top and bottom halves of the tetramer. In contrast, hybrid tetramers, which have functional AMP binding sites in only one half (top/bottom), exhibit an R- to T-state transition and complete AMP inhibition, but without cooperativity. Evidently, two pathways of allosteric inhibition of fructose-1,6-bisphosphatase are possible, only one of which is cooperative.

Disciplines

Biochemistry | Chemistry | Molecular Biology

Hybrid Tetramers of Porcine Liver Fructose-1,6-bisphosphatase Reveal Multiple Pathways of Allosteric Inhibition*

Scott W. Nelson, Richard B. Honzatko, and Herbert J. Fromm‡

From the Department of Biochemistry, Biophysics, and Molecular Biology, Iowa State University, Ames, Iowa 50011

Fructose-1,6-bisphosphatase is a square planar tetramer of identical subunits, which exhibits cooperative allosteric inhibition of catalysis by AMP. Protocols for *in vitro* subunit exchange provide three of five possible hybrid tetramers of fructose-1,6-bisphosphatase in high purity. The two hybrid types with different subunits in the top and bottom halves of the tetramer co-purify. Hybrid tetramers, formed from subunits unable to bind AMP and subunits with wild-type properties, differ from the wild-type enzyme only in regard to their properties of AMP inhibition. Hybrid tetramers exhibit cooperative, potent, and complete (100%) AMP inhibition if at least one functional AMP binding site exists in the top and bottom halves of the tetramer. Furthermore, titrations of hybrid tetramers with AMP, monitored by a tryptophan reporter group, reveal cooperativity and fluorescence changes consistent with an R- to T-state transition, provided that again at least one functional AMP site exists in the top and bottom halves of the tetramer. In contrast, hybrid tetramers, which have functional AMP binding sites in only one half (top/bottom), exhibit an R- to T-state transition and complete AMP inhibition, but without cooperativity. Evidently, two pathways of allosteric inhibition of fructose-1,6-bisphosphatase are possible, only one of which is cooperative.

Fructose-1,6-bisphosphatase (D-fructose-1,6-bisphosphate 1-phosphohydrolase, EC 3.1.3.11; FBPase)[1] catalyzes the hydrolysis of fructose 1,6-bisphosphate ($F16P_2$) to fructose 6-phosphate (F6P) and inorganic phosphate (P_i) (1, 2). FBPase, a key regulatory enzyme of the gluconeogenic pathway, is itself regulated indirectly through the action of glucagon and insulin and directly by the ligation of AMP and $F26P_2$. AMP and $F26P_2$ inhibit FBPase while simultaneously activating its counterpart in glycolysis, fructose-6-phosphate 1-kinase (3, 4). AMP binds 28 Å away from the nearest active site, and noncompetitively inhibits catalysis with respect to $F16P_2$ but competitively in-

hibits with respect to essential divalent cations (Mg^{2+}, Mn^{2+}, or Zn^{2+}) (5–7). $F26P_2$ enhances the binding of AMP up to an order of magnitude (8). Hormonal control of the biosynthesis and degradation of $F26P_2$ facilitates regulation of glycolysis and gluconeogenesis through the coordinated modulation of fructose-6-phosphate 1-kinase and FBPase activities (4, 9).

FBPase is a homotetramer (subunit M_r of 37,000 (10)) and exists in at least two distinct quaternary conformations called R and T (11, 12). AMP induces the transition from the active R-state to the inactive (or less active) T-state. Substrates or products in combination with metal cations stabilize the R-state conformation. A proposed mechanism for allosteric regulation of catalysis involves three conformational states of loop 52–72 called engaged, disengaged, and disordered (13). AMP, alone or with $F26P_2$, stabilizes a disengaged loop (14, 15), whereas metals with products stabilize an engaged loop (15, 16). The enzyme is active if loop 52–72 can cycle between its engaged and disordered conformations. Fluorescence from a tryptophan reporter group at position 57 is consistent with the conformational states for loop 52–72, observed in crystal structures (17, 18). Presumably, the engaged, disengaged, and disordered conformations of loop 52–72 are possible in both the R- and T-states of FBPase, but only the engaged and disordered conformers of the R-state, and the disengaged conformer of the T-state, have been reported in crystalline complexes (16, 19, 20).

A central question remains concerning the allosteric regulation of FBPase: By what mechanism does AMP cooperativity occur in the allosteric inhibition of FBPase? Lipscomb and colleagues (21) have described potential routes of AMP communication across two different subunit interfaces (C1 to C4 and C1 to C2; Fig. 1). In addition, interactions of the N-terminal segment could provide yet another pathway of communication between subunits C1 and C2 (19). Mutations of residues throughout the enzyme, including both interfaces and loop 52–72, have eliminated AMP cooperativity. In many instances, however, significant changes in kinetic parameters and/or mechanisms that accompany the loss of AMP cooperativity thwart definitive conclusions.

Hetero-oligomers, or hybrids, of an otherwise homo-oligomeric protein can be used to great advantage in dissecting mechanisms of thermodynamic coupling between ligands. Hybrid constructs of aspartate carbamoyltransferase have revealed pathways of signal propagation and conformational changes due to the binding of allosteric effectors (22–25). Hybrid enzymes of lactate dehydrogenase from *Bifidobacterium longum* have demonstrated a concerted transition between the R- and T-states of that enzyme (26, 27).

On the basis of previous work, distinct homotetramers of FBPase, when combined under the appropriate conditions, undergo spontaneous subunit exchange to form hybrid tetramers. Anion-exchange chromatography cleanly separates most of the

---

[1] The abbreviations used are: FBPase, fructose-1,6-bisphosphatase; $F16P_2$, fructose 1,6-bisphosphate; F6P, fructose 6-phosphate; $F26P_2$, fructose 2,6-bisphospate; P_i, orthophosphate; AMP^-, triple mutation $Tyr^{113} \rightarrow Phe/Lys^{112} \rightarrow Met/Thr^{31} \rightarrow Val$; Glu-tagged, C-terminal extension of 9 glutamic acid residues; HPLC, high performance liquid chromatography; CD, circular dichroism; FMP, formycin A 5'-monophosphate.
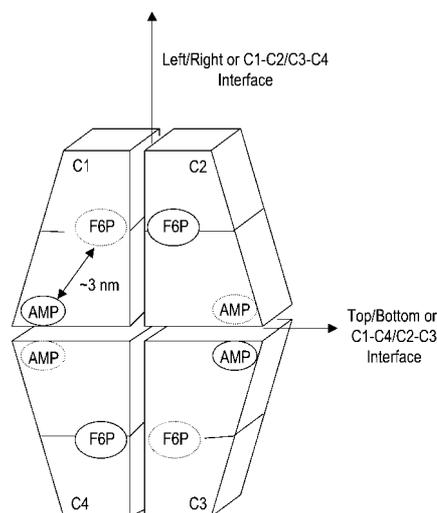
FIG. 1. **Schematic of FBPase showing subunit and interface nomenclature.** Active sites and AMP binding sites are labeled F6P and AMP, respectively. *Dashed circles* represent ligand binding sites on the face hidden from view.

hybrid constructs (28). More recently, Kantrowitz and colleagues (29) reported that AMP must bind to two subunits of FBPase to cause significant inhibition. They were unable to investigate the origin of AMP cooperativity, however, because their system was an unresolved mixture of three distinct 2:2 hybrid tetramers (29). Our motivation for developing an *in vitro* subunit exchange protocol lay in its potential to exercise control over the formation and separation of hybrid tetramers. As distinct 2:2 hybrids can be isolated by protocols presented here, specific pathways of cooperativity can be tested. The kinetic and equilibrium binding data presented here show that one molecule of AMP must bind to each half (top/bottom) of the FBPase tetramer to promote cooperative AMP inhibition; however, AMP molecules bound to the same half of the tetramer can still elicit complete allosteric inhibition without cooperativity. Furthermore, the ligation of AMP molecules to any pair of subunits of the tetramer will promote an R- to T-transition.

EXPERIMENTAL PROCEDURES

Materials—$F16P_2$, $F26P_2$, $NADP^+$, and AMP were purchased from Sigma. Glucose-6-phophate dehydrogenase and phosphoglucose isomerase came from Roche Molecular Biochemicals. Other chemicals were of reagent grade or the equivalent. QSW-HR HPLC resin was from Toso-Hass Bioseparations. The FBPase-deficient *Escherichia coli* strain DF 657 came from the Genetic Stock Center at Yale University. Plasmids used in the expression of wild-type and $Tyr^{57} \rightarrow Trp$ FBPases came from a previous investigation (17, 18). Sigma Genosys provided all oligonucleotides used in directed mutations.

Mutagenesis of Wild-Type FBPase—Mutations were accomplished by deletion of or specific base changes in double-stranded plasmids using the QuikChange site-directed mutagenesis kit (Stratagene). The following FBPases were developed in the context of work presented here: (i) Glu-tagged (the wild-type subunit with an extension of 9 glutamic acid residues to its C terminus), (ii) $Tyr^{113} \rightarrow Phe$ mutant, (iii) $Tyr^{113} \rightarrow Phe/Lys^{112} \rightarrow Met$ double mutant, (iv) AMP^- (the $Tyr^{113} \rightarrow Phe/Lys^{112} \rightarrow Met/Thr^{31} \rightarrow Val$ triple mutant), (v) $Gly^{26} \rightarrow Ile/Thr^{27} \rightarrow Asp$ double mutant, and (vi) AMP^-/Trp^{57} (the $Tyr^{113} \rightarrow Phe/Lys^{112} \rightarrow Met/Thr^{31} \rightarrow Val/Tyr^{57} \rightarrow Trp$ quadruple mutant). The mutations and integrity of the resulting genes were confirmed by sequencing the promoter region and the entire open reading frame. The Iowa State University sequencing facility provided DNA sequences using the fluorescent dye-dideoxy terminator method.

Expression and Purification of Wild-type and Mutant Homotetramers—All of the FBPases were expressed in a strain of *E. coli* deficient in endogenous FBPase and then purified to homogeneity. Cell-free extracts of the wild-type and Glu-tagged FBPases were subjected to heat treatment (65 °C for 5 min), followed by centrifugation. The supernatant solution was loaded onto a Cibacron Blue-Sepharose column, pre-

viously equilibrated with 20 mM Tris-HCl, pH 7.5. FBPases were eluted from that column with 1 mM AMP and 20 mM Tris-HCl, pH 7.5. The eluent was loaded directly onto a DEAE-Sepharose column and eluted with a gradient of NaCl from 0–0.3 M. Constructs ii–vi above (all of which were impaired with respect to AMP binding) were purified as above, but using instead a NaCl gradient from 0–0.7 M to elute proteins from the Cibacron Blue column. These AMP-impaired FBPases required an additional step of purification using phosphocellulose chromatography. A phosphocellulose column was equilibrated against 20 mM Tris-HCl, pH 7.5, and the above enzymes were eluted with 5 mM $F16P_2$ and 20 mM Tris-HCl, pH 7.5. All proteins were dialyzed extensively against 20 mM Tris-HCl, but FBPases with impaired AMP binding (constructs ii–vi above) were dialyzed first against 1 mM $MgCl_2$, followed by 20 mM Tris-HCl. The latter procedure removed $F16P_2$ introduced during phosphocellulose chromatography. Protein purity and concentration was confirmed by SDS-polyacrylamide gel electrophoresis (30) and the Bradford assay (31), respectively.

Formation and Purification of Hybrid Enzymes—Hybridization protocols developed here employed only pure FBPases. Appropriate enzymes were combined overnight at 4 °C, after which the mixture was loaded onto a QSW-HR HPLC column, previously equilibrated with 20 mM Tris-HCl, pH 7.5. Individual hybrids were eluted with 20 mM Tris-HCl, pH 7.5, and a gradient from 0 to 0.3 M in NaCl. The nomenclature of 2:2 hybrids used here is that of Cornish-Bowden and Koshland (32). The letters p, q, and r refer to 2:2 hybrids with like subunits at positions C1/C2, C1/C4, and C1/C3 of the tetramer, respectively (Fig. 2). Differences in electrostatic charge of various tetramers due to different numbers of polyglutamyl tags permitted the partial assignment of peaks in the elution profile to specific hybrids that formed from protocol A of Fig. 2. Retention times should increase with the number of Glu-tagged subunits in a tetramer. Indeed, the retention times of pure wild-type homotetramer and pure Glu-tagged homotetramer correspond to those of the first and last peaks eluted from hybrid mixtures. The second and penultimate peaks were assigned to 3:1 hybrids (3 subunits wild-type to 1 subunit Glu-tagged) and to 1:3 hybrids (1 subunit wild-type to 3 subunits Glu-tagged), respectively. The three possible 2:2 hybrids resolved into two peaks. Assignments of hybrid type to these peaks entailed hybridization protocols B and C of Fig. 2. In the presence of $F16P_2$, subunit exchange occurs only at the level of C1/C2 dimers (28). Hence, protocol B leads to hybrids 4:0, 0:4, and 2:2p. The corresponding elution profile has but three peaks, the assignment of two of which (hybrids 4:0 and 0:4) is unambiguous. The central peak of the elution profile of protocol B, which must be the 2:2p hybrid, corresponds in retention time to one of two 2:2 hybrid peaks from the elution profile of protocol A. Using a similar process protocol C leads to a mixture of 2:2q and 2:2r hybrids. The corresponding elution profile again has three peaks, with the third peak being unambiguously due to the mixture of 2:2q/2:2r hybrids. The retention time of the 2:2q/2:2r hybrids from protocol C corresponds to the other 2:2 hybrid peak of protocol A. To arrest subunit exchange in purified hybrid enzymes, the hybrids were kept at room temperature (which slows subunit exchange). All kinetics and fluorescence experiments were performed within 3 h of hybrid purification. After the assays had been performed, hybrid enzymes were checked with nondenaturing polyacrylamide gel electrophoresis to ensure the absence of subunit exchange.

Circular Dichroism Spectroscopy—Circular dichroism spectra were recorded for wild-type and mutant FBPases at room temperature on a Jasco J710 CD spectrometer in a 1-cm cell, using a protein concentration of 0.35 mg/ml. Spectra were collected from 200 to 260 nm in increments of 1.3 nm. The spectra analyzed were an average of three independent scans. Each spectrum was blank-corrected using the software package provided with the instrument.

Kinetic Experiments—Assays for the determination of specific activity, k_{cat}, and activity ratios at pH 7.5 and 9.5 employed the coupling enzymes, phosphoglucose isomerase and glucose-6-phosphate dehydrogenase (1). The reduction of $NADP^+$ to NADPH was monitored by absorbance spectroscopy at 340 nm. All other assays used the same coupling enzymes but monitored NADPH production by its fluorescence emission at 470 nm, using an excitation wavelength of 340 nm. Kinetic assays were performed at room temperature (22 °C). Initial kinetic rates were analyzed using programs written either in the MINITAB language, using an α value of 2.0 (33), or by the ENZFITTER program (34).

Steady-state Fluorescence Measurements—Fluorescence data were collected using an SLM 8100C Spectrofluorometer from Spectronic Instruments. The single tryptophan at position 57 was excited selectively using a wavelength of 295 nm. Fluorescence emission spectra were recorded in steps of 1 nm from 310 to 400 nm with a slit width of 2 nm

FIG. 2. **Protocols for hybridization and the assignment of hybrid types to elution profiles.** *A*, general method provides all possible hybrid tetramers between AMP$^-$ and Glu-tagged homotetramers. *B*, special method for generating the 2:2p hybrid tetramer without 2:2q and 2:2r hybrid tetramers. *C*, special method for generating 2:2q and 2:2r hybrid tetramers without the 2:2p hybrid tetramer. *Shaded polygons* represent subunits with nonfunctional AMP sites (AMP$^-$), and *open polygons* with *dotted extensions* represent Glu-tagged subunits. Corresponding elution profiles and retention times are immediately *below* each protocol. Peaks marked with *arrows* represent inactive protein (FBPase activity in the elution profile for A is given by the *dotted line* and *solid diamonds*). These peaks can be significant (as shown) or be absent from the elution profile and are presumably unfolded and/or aggregated subunits of FBPase.
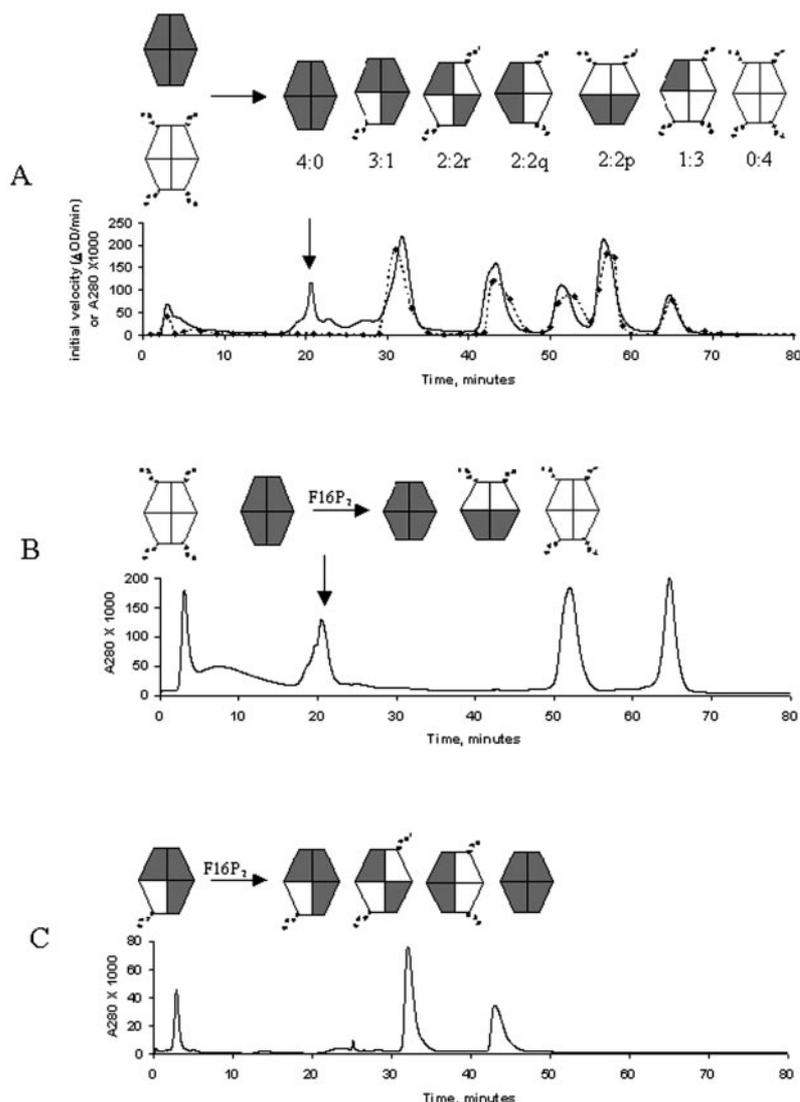
for both excitation and emission. The spectra presented are the average of three scans. Enzyme concentrations ranged from 0.2 to 0.3 mg/ml. As a control, the highest concentration of AMP used here caused no change in fluorescence emission from a solution of tryptophan (100 μM) or from the AMP$^-$/Trp[57] homotetramer.

AMP titration data were analyzed by nonlinear least squares fits, using the following equation,

$$\frac{\Delta F}{F_o} = \frac{(\Delta F_{max}/F_o) \times L^n}{K_d + L^n} \qquad (\text{Eq. 1})$$

where ΔF_{max} is the change in fluorescence caused upon addition of ligand L, F_o is the fluorescence in the absence of ligand, K_d is the dissociation constant, and n is the Hill coefficient.

RESULTS

Expression and Purification of Wild-type and Mutant Homotetramers—Expression and isolation procedures described above provided homotetramers of FBPase at least 95% pure by SDS-polyacrylamide gel electrophoresis (data not shown). AMP-impaired FBPases (constructs ii–vi described above) did not elute from the Cibacron blue column, using AMP concentrations up to 20 mM. A gradient in NaCl successfully eluted these enzymes, but an additional purification step (phosphocellulose chromatography) was necessary to achieve at least 95% purity.

Formation and Purification of Hybrid Tetramers—Subunit exchange between Glu-tagged (9-residue polyglutamyl exten-

sion to the C terminus) and AMP$^-$ homotetramers, and between Glu-tagged and AMP$^-$/Trp[57] homotetramers, occurs at rates comparable to that of Glu-tagged and wild-type homotetramers. By the strategy presented under "Experimental Procedures," peaks with retention times of ~43 and 52 min (Fig. 2) correspond to a mixture of 2:2q and 2:2r hybrids and to a pure 2:2p hybrid, respectively (Fig. 3). The kinetic properties of the 2:2p hybrid created by protocol A or B (Fig. 2) are quantitatively identical. Over several preparations, the 2:2q/2:2r hybrid mixtures from protocols A and C differ reproducibly but not to a statistically significant extent. The 2:2q/2:2r hybrid mixture from protocol A has a lower Hill coefficient for AMP (1.4 $\pm$ 0.1) and a higher IC$_{50}$ (11.3 $\pm$ 0.8) than that exhibited by the 2:2q/2:2r hybrid mixture from protocol C (Table I). Because the relative amounts of Glu-tagged and AMP$^-$ subunits are different in protocols A and C, and because protocol C employs F16P$_2$, whereas protocol A does not, the relative amounts of 2:2q and 2:2r need not be the same for each protocol.

Secondary Structure Analysis—The CD spectra of all homotetramers and hybrids are identical from 200 to 260 nm (data not shown), indicating little or no effect on the secondary structure of FBPase due to mutations and hybridization protocols.

Kinetics Experiments—Kinetic parameters of wild-type, Glu-tagged, AMP$^-$, and Tyr[57] $\rightarrow$ Trp homotetramers, as well as
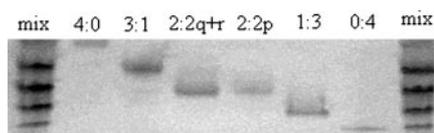
FIG. 3. **Nondenaturing polyacrylamide electrophoresis gel of purified hybrids.** The names of the hybrids are *above the lane.* Tetramer hybrids 2:2q/2:2r and 2:2p each have two Glu-tags but have different retention times in HPLC separations as demonstrated in Fig. 2.

specific hybrids from subunit exchange between Glu-tagged and AMP⁻ homotetramers are given in Table I. The Glu-tag does not perturb functional properties as evidenced by the nearly identical kinetic parameters for the wild-type and Glu-tagged homotetramers. The AMP⁻ homotetramer exhibits nearly a 12,000-fold decrease in AMP inhibition and some loss of AMP cooperativity with no change in any other kinetic property. The mechanism of AMP inhibition for the AMP⁻ homotetramer is uncertain. AMP may bind to the active site, and/or Na⁺ introduced along with the AMP may displace Mg^{2+} from the active site. Hence, the observed cooperativity (Hill coefficient of 1.4; Table I) for this low affinity interaction probably arises from a mechanism entirely different from that of the high affinity AMP inhibition. Other homotetramers, not fully characterized kinetically, revealed IC_{50} values for AMP of 4, 6, and 3 mM for Tyr¹¹³ → Phe, Tyr¹¹³ → Phe/Lys¹¹² → Met, and Gly²⁶ → Ile/Thr²⁷ → Ile FBPases, respectively. The later double mutation confirms speculation regarding the loss of AMP recognition by chloroplast FBPases (35). The Gly²⁶ → Ile/Thr²⁷ → Ile mutations create a chloroplast "AMP" pocket within the context of the porcine liver enzyme and a concomitant rise (3000-fold) of IC_{50} relative to that of the wild-type enzyme. The AMP⁻ homotetramer was used in subsequent subunit exchange experiments, because it has the highest IC_{50} for AMP while preserving all other kinetic properties of the wild-type enzyme.

Experiments in kinetics were performed immediately following the purification of hybrid enzymes. Hybrid tetramers were stable for several hours at 25 °C (but not at 4 °C). All the kinetic parameters of the hybrids were essentially identical to those of the wild-type enzyme, except those for AMP inhibition (Table I).

Inhibition of Hybrid Tetramers by AMP—IC_{50} for the 2:2p hybrid is ∼40 μM with a Hill coefficient of 1.0. Inhibition is complete upon saturation of the two high affinity AMP binding sites (Figs. 4 and 5). In contrast, AMP inhibition of the 2:2q/2:2r hybrid mixture is cooperative and 100% at saturation. The 2:2q/2:2r hybrid mixture has an IC_{50} of 6.1 μM with a Hill coefficient for AMP of 1.5. The hybrid enzyme with three functional AMP binding sites and a single AMP-impaired binding site (1:3 hybrid, Fig. 2) responds to AMP much like the 2:2q/2:2r hybrid mixture with a Hill coefficient of 1.6 and an IC_{50} for AMP of 6.8 μM.

Steady-state Fluorescence—AMP-induced changes in the fluorescence of hybrid FBPases are due to conformational changes in loop 52–72 of subunits, which do not possess functional AMP binding sites. Hence, the reporter groups sense conformational change due to AMP ligation of a neighboring subunit. This conformational change is most likely the transition from R- to T-state FBPase.

Fluorescence spectra of Trp⁵⁷ FBPase (Fig. 6) are consistent with three conformational states of loop 52–72, observed in previous work (17, 18). All hybrids exhibit identical fluorescence spectra in the presence of products and divalent cations (R-state, loop engaged), and in the absence of all ligands (R-state, loop disordered). Hybrids 0:4, 1:3, 2:2p, and 2:2q/2:2r are

sensitive to AMP, and at saturating levels of AMP attain nearly equivalent fluorescence spectra. In contrast, the fluorescence spectrum of AMP⁻/Trp⁵⁷ hybrids 3:1 and 4:0 are insensitive to AMP. Evidently, loops 52–72 of these FBPase hybrids cannot achieve the T-state, disengaged loop conformation.

Changes in fluorescence in response to the titration of AMP confirm the absence of cooperativity in 2:2p hybrid tetramer and the existence of cooperativity in AMP-ligation of the 2:2q/2:2r and 1:3 hybrid tetramers (Table II). Dissociation constants determined by fluorescence spectroscopy mirror the variation in IC_{50} values. The K_d values for the 2:2q/2:2r and 1:3 hybrids are substantially lower than that of the 2:2p hybrid tetramer.

DISCUSSION

Kinetic parameters (k_{cat}, ratio of activities at pH 7.5 and 9.5, K_m for F16P₂, K_a for Mg^{2+}, Hill coefficient for Mg^{2+}, and K_i for F26P₂) and kinetic mechanisms of inhibition are virtually identical for hybrid and wild-type enzymes (Table I). Henceforth the discussion will focus on the two phenomena that differ: AMP cooperativity and AMP inhibition.

Cooperativity can be a property of the entire oligomer, in which case the Hill coefficient varies smoothly with the number of functional ligand binding sites in hybrid constructs. Such is the case for hybrids of lactate dehydrogenase from *Bacillus longum* (26). On the other hand, if the mechanism of cooperativity relies on the integrity of a specific subunit interface, then mutations at that interface should eliminate cooperativity, whereas mutations elsewhere should have no effect. Cooperativity in the binding of NAD to tetrameric glyceraldehyde-3-phosphate dehydrogenase, for instance, is sensitive to the O–P interface (36).

Neither of these scenarios, however, applies to FBPase. The lack of cooperativity in AMP inhibition of the 2:2p hybrid indicates no participation by the C1–C2 interface in this phenomenon. On the other hand, the 0:4 hybrid (Glu-tagged homotetramer) and the 1:3 hybrid (1 subunit AMP⁻:3 subunits Glu-tagged) have Hill coefficients for AMP of 2.0 and 1.6, respectively, suggesting some correlation between the number of functional binding sites and the Hill coefficient. If 2:2 hybrids can have cooperativity no greater than that of the 1:3 hybrid, then the Hill coefficient of 1.5 for the 2:2q/2:2r hybrid mixture requires either one of the hybrids (2:2q or 2:2r) is dominant and cooperative or that both hybrids are cooperative.

Of the two possibilities, mentioned above, the latter is most probable. To have the formation of say the 2:2q hybrid, but not the 2:2r hybrid, requires either a bias in the equilibrium distribution of hybrids or a bias in the kinetics of subunit exchange. Although the relative areas of peaks in the elution profile of Fig. 2*A* are not consistent with a binomial distribution, we see no evidence that would suggest a thermodynamic bias so large as to exclude the formation of any specific hybrid. Furthermore, we can envision a mechanism of subunit exchange that discriminates against the formation of both hybrids 2:2q and 2:2r, but no mechanism that leads to the formation of just one of these hybrids. Therefore, the data here infer comparable levels of each hybrid in the 2:2q/2:2r mixture and, hence, that both the 2:2q and 2:2r hybrids must have nearly equal AMP cooperativity.

Directed mutations that alter AMP cooperativity in a homotetramer of FBPase generally do not support a definitive conclusion regarding the mechanism of cooperativity (37–42). Mutations of Arg⁴⁹ or Lys⁵⁰ (residues located at the C1–C2 interface) eliminate AMP cooperativity (41, 42), but they also change the kinetic mechanism of AMP inhibition from noncompetitive to uncompetitive with respect to F16P₂ and from competitive to noncompetitive with respect to Mg^{2+}. One can infer little regarding cooperativity in a kinetic mechanism, if the

TABLE I

Kinetic parameters for wild-type, mutant, and hybrid FBPases

The names of the FBPases are defined under "Experimental Procedures" and Fig. 2.

FBPase	Activity ratio[a]	k_{cat}[b]	K_m-F16P$_2$[c]	K_a-Mg^{2+}	Hill coeff. Mg^{2+}[d]	K_i-F26P$_2$[c]	IC$_{50}$-AMP[e]	Hill coeff. AMP
		s^{-1}	μM	mM^2		μM	μM	
Wild-type	3.3	22 ± 1	1.8 ± 0.1	0.67 ± 0.04	1.9 ± 0.1	0.12 ± 0.01	1.61 ± 0.05	2.2 ± 0.1
Trp[57]	3.3	24 ± 1	3.4 ± 0.1	0.53 ± 0.06	1.9 ± 0.1	0.84 ± 0.05	8.5 ± 0.4	2.1 ± 0.1
Glu-tagged	3.5	23 ± 1	2.2 ± 0.1	0.65 ± 0.05	2.1 ± 0.1	0.11 ± 0.01	1.4 ± 0.1	2.0 ± 0.1
1:3	3.5	22 ± 2	2.2 ± 0.2	0.35 ± 0.03	2.2 ± 0.1	0.16 ± 0.02	6.1 ± 0.3	1.6 ± 0.1
2:2q/2:2r	3.3	21 ± 1	1.8 ± 0.1	0.59 ± 0.04	2.0 ± 0.1	0.15 ± 0.01	6.8 ± 0.5	1.5 ± 0.1
2:2p	3.4	23 ± 2	1.7 ± 0.1	0.41 ± 0.05	2.0 ± 0.1	0.183 ± 0.02	43 ± 2	0.99 ± 0.05
3:1	3.2	22 ± 1	1.8 ± 0.2	0.39 ± 0.02	2.2 ± 0.1	0.20 ± 0.01	340 ± 10[f]	1.00 ± 0.04
AMP$^-$	3.2	21 ± 1	2.7 ± 0.1	0.46 ± 0.03	2.1 ± 0.1	0.15 ± 0.01	11700 ± 600	1.4 ± 0.1

[a] Ratio of specific activities at pH 7.5 and 9.5.

[b] Determined at saturating substrate concentrations.

[c] Determined at a Mg^{2+} concentration of 5 mM.

[d] Determined at an F16P$_2$ concentration of 20 μM.

[e] Determined at a Mg^{2+} concentration equal to the K_a-Mg^{2+} of each enzyme and a F16P$_2$ concentration of 20 μM.

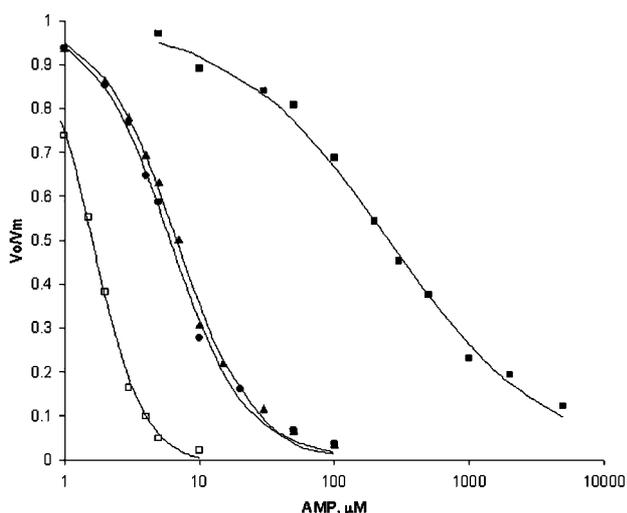[f] Value calculated using normalized data shown in the inset of Fig. 5.

FIG. 4. **Response of potently and completely inhibited FBPases to AMP.** *Curves* represent wild-type (□), 1:3 (●), 2:2q/2:2r (▲), and 2:2p (■) FBPases. The inhibition assays were performed in 20 μM F16P$_2$ and 0.5 mM Mg^{2+}.

mechanism itself is changed by the experiment. Indeed, the mutation of Lys[50] to methionine has no effect on kinetic mechanisms and little or no effect on kinetic parameters, including AMP cooperativity (41). Mutations of Arg[49] and Lys[50] that result in significant functional perturbations are due most likely to their influence on the conformational dynamics of loop 52–72. Mutations of Asn[64], Asp[74], and Glu[98], residues in or near loop 52–72, eliminate AMP cooperativity (43, 44). The introduction of proline at position 50 dramatically alters the mechanism of AMP inhibition and, on the basis of fluorescence spectroscopy, greatly changes the conformational dynamics of loop 52–72 (45). In contrast, the 2:2p hybrid preserves all of the kinetic properties of the wild-type enzyme, save AMP cooperativity.

There are, however, mutations that eliminate AMP cooperativity with only modest effects on other kinetic parameters. Mutations of Lys[42], Ile[190], Gly[191], and Glu[192] (residues at the C1–C4 interface) are such examples (39, 40). The above mutants of FBPase exhibit biphasic inhibition by AMP: maximal inhibition of substantially less than 100% at low concentrations of AMP (<10 μM), followed by complete inhibition at concentrations of AMP >10 mM. Lu *et al.* (38) concluded that such biphasic AMP inhibition is a consequence of lost AMP cooperativity. The 2:2p hybrid, however, has no AMP cooperativity and no biphasic AMP inhibition. An alternative model by Nel-

son *et al.* (13) accounts for biphasic AMP inhibition as a failure to stabilize the disengaged conformation of loop 52–72. Hence, catalysis in the presence of AMP arises from the T-state of FBPase, and the observed maximal inhibition at low concentrations of AMP is due to the transition from an active R-state to a less active T-state. The later model accounts for biphasic AMP inhibition but says nothing regarding the mechanism of AMP cooperativity.

Of the several mutations that eliminate AMP cooperativity in homotetramers of FBPase, the mutation of Arg[22] to methionine perhaps makes the most compelling case for the participation of a specific subunit interface in the mechanism of AMP cooperativity. Met[22] FBPase exhibits no cooperativity in AMP inhibition yet retains all other wild-type kinetic mechanisms and parameters (37). Arg[22] (of subunit C1) hydrogen bonds with backbone carbonyl 27 (of subunit C4) in the T-state of wild-type FBPase. This intersubunit hydrogen bond is absent, however, in the R-state. The absence of AMP cooperativity in Met[22] FBPase implicates the top/bottom (C1–C4/C2–C3) interface in the phenomenon. As the top/bottom interface extends the entire width of the FBPase tetramer (Fig. 1), the coupling mechanism responsible for cooperativity can involve any pair of AMP molecules bound to opposite sides of the interface. The observation of cooperativity in the 2:2q/2:2r hybrid mixture and its absence in the 2:2p hybrid is fully consistent with a mutation that evidently severs communications between the top and bottom halves of the FBPase tetramer.

Although AMP cooperativity may not be inseparably linked to allosteric inhibition, as noted above, AMP affinity and cooperativity are correlated phenomena. Cooperativity is highest and IC$_{50}$ for AMP is lowest in the 0:4 hybrid (Glu-tagged homotetramer). As the number of AMP$^-$ subunits increases in the hybrid, the Hill coefficient declines and IC$_{50}$ for AMP rises. The 1:3 hybrid and the 2:2q/2:2r hybrid mixture are the exceptions to this trend. In fact, the kinetic properties of the 1:3 hybrid and 2:2q/2:2r hybrid mixture are nearly identical, whereas the 2:2p hybrid has no cooperativity and an IC$_{50}$ for AMP some 6-fold higher. Evidently, potent and cooperative AMP inhibition of FBPase requires at least one AMP molecule bound to each half (top/bottom) of the tetramer. This finding is in harmony with evidence for pairs of high and low affinity sites for AMP on wild-type FBPase (46).

The fluorescence data infer a common R-state conformation for hybrids and a global conformational change induced by saturating concentrations of AMP. The Trp[57] reporter group behaves as if the 1:3 and 2:2 hybrids are undergoing the same R- to T-state transition as observed in the wild-type enzyme. The 12-fold rise in K_d for AMP, exhibited by the 2:2p hybrid

FIG. 5. **Response of weakly inhibited FBPases to AMP.** *Curves* represent 3:1 (♦) and AMP⁻ (▲) FBPases. The inhibition assays were performed in 20 μM F16P$_2$ and 0.5 mM Mg^{2+}. *Inset*, the curve for the 3:1 tetramer hybrid less the calculated AMP inhibition based on the curve for the AMP⁻ homotetramer. The "corrected" curve reveals the specific effect due to the high affinity association of AMP with the single functional subunit of the 3:1 hybrid tetramer.
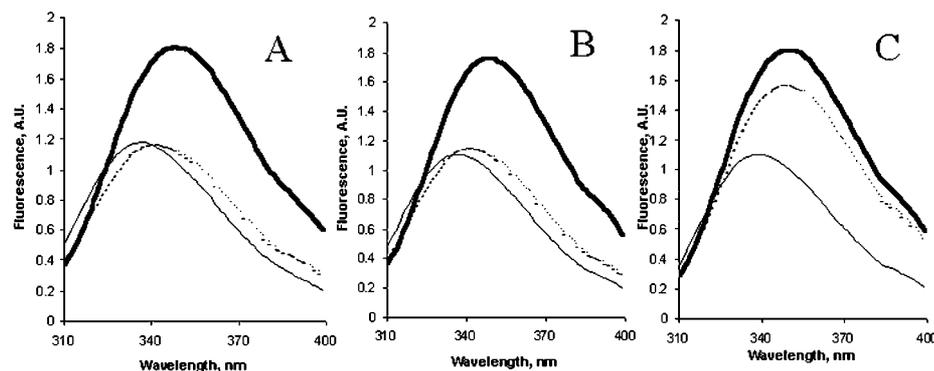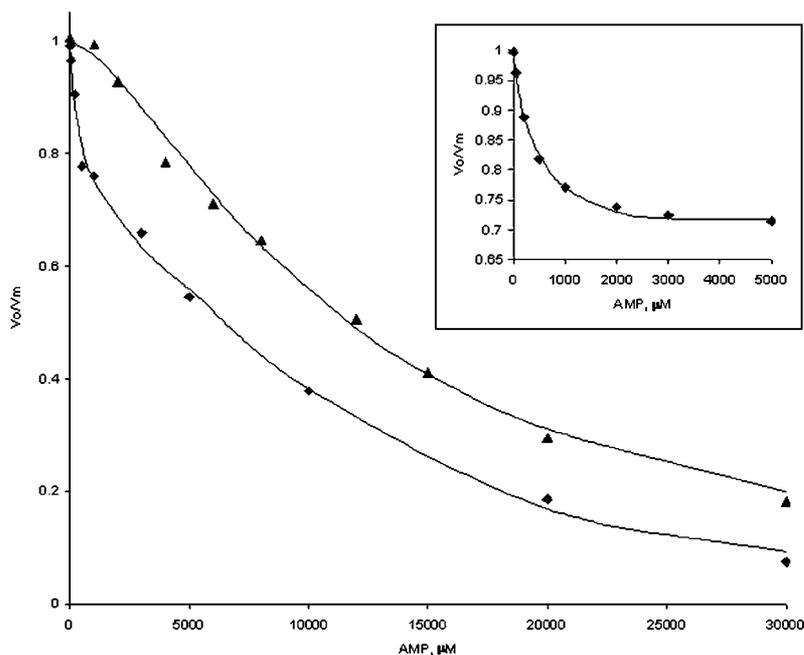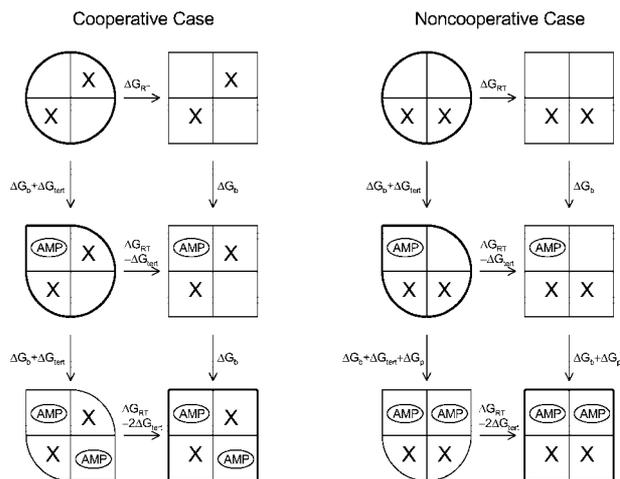

FIG. 6. **Fluorescence spectra of representative tetramer hybrids formed from AMP⁻/Trp^{57} and Glu-tagged homotetramers.** *Bold lines* represent conditions (5 mM KP$_i$, 5 mM F6P, and 50 μM ZnCl$_2$) under which the wild-type enzyme is in its R-state, loop-engaged conformation. *Thin lines* represent the apo enzyme (no ligands or metals present). *Dashed lines* represent conditions (5 mM KP$_i$, 5 mM F6P, 50 μM ZnCl$_2$, and 1 mM AMP) under which the wild-type enzyme is in its T-state, loop disengaged conformation. *A* is the 2:2p hybrid tetramer, *B* is the 2:2q+r hybrid tetramers, and *C* is the 3:1 hybrid tetramer.

TABLE II
Dissociation constants and Hill coefficients for AMP⁻/Trp^{57} FBPase hybrids
Corresponding data provided for Trp^{57} FBPase from Ref. 17.

FBPase	K_d	Hill coefficient
Trp^{57}	17 ± 1	2.1 ± 0.1
1:3	21.2 ± 0.8	1.60 ± 0.09
2:2q/2:2r	42 ± 3	1.5 ± 0.1
2:2p	210 ± 10	1.0 ± 0.1
3:1	400 ± 70	0.8 ± 0.1

FIG. 7. **Thermodynamics of cooperative (*left*) and noncooperative (*right*) inhibition of 2:2 hybrid tetramers of FBPase by AMP.** Free energy terms ΔG_b, ΔG_{tert}, ΔG_{RT}, and ΔG_p are defined in the text. AMP cannot bind to subunits with *crosses*. R-state subunits are *rounded*, whereas T-state subunits have *corners*. Predominant forms of the tetramer in solution at equilibrium are represented with *bold outlines*.

relative to the Trp^{57} homotetramer, reflects most likely the diversion of more AMP binding energy to promote the R- to T-state transition. Hence, one molecule of AMP ligated to each half (top/bottom) of the tetramer is more effective in driving the R- to T-state transition, than a pair of AMP molecules bound to the same half of the tetramer. A 3:1 hybrid (3 subunits AMP⁻:1 subunit Glu-tagged) of FBPase is poorly inhibited by AMP (IC$_{50}$ of 340 μM) and, on the basis of fluorescence spectroscopy, cannot drive the R- to T-transition. Data here from thermodynamics and kinetics then are in substantial agreement: Potent and cooperative inhibition of FBPase occurs by the binding of one AMP molecule to each of the bottom and top halves of the tetramer, driving an R- to T-state transition.

These findings indicate two possible pathways of allosteric inhibition: a cooperative pathway, triggered by the binding of a pair of AMP molecules to opposites sides of the top/bottom interface, and a noncooperative pathway, triggered by the binding of a pair of AMP molecules to the same side of the top/bottom interface. Given the relative IC$_{50}$ values for AMP inhibition of the 2:2 hybrid tetramers, AMP prefers binding to opposite sides of the top/bottom interface. Formycin A 5′-mono-

phosphate (FMP) and 2′(3′)-*O*-(trinitrophenyl)adenosine 5′-monophosphate, however, cause complete allosteric inhibition with no cooperativity (7, 45). For reasons unknown, the later effectors may prefer binding to the same side of the top/bottom interface of the wild-type tetramer, and thus the absence of cooperativity in allosteric inhibition. Crystal structures of human FBPase, fully ligated with AMP and with FMP, however, reveal no discernable differences (47). Hence, differences in AMP and FMP complexes of FBPase must lie in partially ligated states of the enzyme, a conclusion at least consistent with the observed functional properties of the 2:2 hybrid tetramers.

Ackers *et al.* (48) have proposed a "symmetry rule" governing the transition of hemoglobin from its T- to R-states. The hemoglobin tetramer is composed of two $\alpha\beta$ dimers. The association of at least one ligand to each of the $\alpha\beta$ dimers of the hemoglobin tetramer favors a T- to R-state transition. In contrast, the R- to T-state transition for FBPase occurs whether ligands bind to opposite halves or to the same half of the tetramer.

How then is it possible for AMP to promote an R- to T-state transition in FBPase with and without cooperativity? A possible explanation appears in Fig. 7, where ΔG_b is the free energy change in the ligation of AMP to an "isolated subunit" of FBPase, ΔG_{tert} is the free energy penalty in overcoming tertiary conformational restraints due to the assembly of the "isolated subunit" into an R-state relative to a T-state tetramer, and ΔG_{RT} is the free energy penalty in overcoming quaternary conformational restraints in the R- to T-state transition. Because unligated and singly ligated tetramers favor the R-state, $\Delta G_{RT} > \Delta G_{tert}$. Because doubly ligated tetramers are in the T-state, however, $2\Delta G_{tert} > \Delta G_{RT}$. The last two inequalities can be combined: $2\Delta G_{RT} > 2\Delta G_{tert} > \Delta G_{RT}$. Cooperative binding of AMP to the 2:2q hybrid tetramer requires only that $\Delta G_b + \Delta G_{tert} > \Delta G_b + \Delta G_{RT} - \Delta G_{tert}$, or equivalently, $2\Delta G_{tert} > \Delta G_{RT}$, which clearly agrees with the relative free energies of unligated, singly ligated, and doubly ligated FBPases.

To account for noncooperative binding of AMP, we assume a thermodynamic penalty (ΔG_p in Fig. 7) in the binding of two AMP molecules to the same half of the tetramer. Such a thermodynamic penalty is consistent with the weaker binding affinity of the third and fourth molecules of AMP to the wild-type tetramer (46). Noncooperative binding of AMP then requires $\Delta G_b + \Delta G_{tert} = \Delta G_b + \Delta G_{RT} - \Delta G_{tert} + \Delta G_p$, or equivalently, $2\Delta G_{tert} = \Delta G_{RT} + \Delta G_p$. This latter equality and the former combined inequality ($2\Delta G_{RT} > 2\Delta G_{tert} > \Delta G_{RT}$) together require only that $\Delta G_{RT} > \Delta G_p > 0$, which is a plausible condition. Hence, the same allosteric effector of FBPase can promote an R- to T-state transition by way of either cooperative or noncooperative binding pathways.

REFERENCES

1. Benkovic, S. T., and de Maine, M. M. (1982) *Adv. Enzymol. Relat. Areas Mol. Biol.* **53,** 45–82
2. Tejwani, G. A. (1983) *Adv. Enzymol. Relat. Areas Mol. Biol.* **54,** 121–194
3. Van Schaftingen, E. (1987) *Adv. Enzymol. Relat. Areas Mol Biol.* **59,** 45–82
4. Pilkis, S. J., El-Maghrabi, M. R., and Claus, T. H. (1988) *Ann. Rev. Biochem.* **57,** 755–783
5. Nimmo, H. G., and Tipton, K. F. (1975) *Eur. J. Biochem.* **58,** 567–574
6. Liu, F., and Fromm, H. J. (1988) *J. Biol. Chem.* **263,** 9122–9128
7. Scheffler, J. E., and Fromm, H. J. (1986) *Biochemistry* **25,** 6659–6665
8. Pilkis, S. J., El-Maghrabi, R. M, McGrane, M. M., Pilkis, J., and Claus, T. H. (1981) *J. Biol. Chem.* **256,** 3619–3622
9. Okar, D. A., and Lange, A. J. (1999) *Biofactors* **10,** 1–14
10. Stone, S. R., and Fromm, H. J. (1980) *Biochemistry* **19,** 620–625
11. Ke, H., Zhang, Y. Liang, J.-Y., and Lipscomb, W. N. (1991) *Proc. Natl. Acad. Sci. U. S. A.* **88,** 2989–2993
12. Liu, F, and Fromm, H. J. (1988) *J. Biol. Chem.* **19,** 9122–9128
13. Nelson, S. W., Kurbanov, F., Honzatko, R. B., and Fromm, H, J. (2001) *J. Biol. Chem.* **276,** 6119–6124
14. Choe, J.-Y., Poland, B. W., Fromm, H. J., and Honzatko, R. B. (1998) *Biochemistry* **33,** 11441–11450
15. Xue, Y., Huang, S., Liang, J.-Y. Zhang, Y., and Lipscomb, W. N. (1994) *Proc. Natl. Acad. Sci. U. S. A.* **91,** 12482–12486
16. Choe, J. Y., Fromm, H. J., and Honzatko, R. B. (2000) *Biochemistry* **39,** 8565–8574
17. Nelson, S. W., Choe, J.-Y., Iancu, C. V., Honzatko, R. B., and Fromm, H. J. (2000) *Biochemistry* **39,** 11100–11106
18. Wen, J., Nelson, S. W., Honzatko, R. B., Fromm, H. J., and Petrich, J. W. (2001) *Photochem. Photobiol.* **74,** 679–685
19. Ke, H. M., Thorpe, C. M., Seaton, B., Lipscomb, W. N., and Marcus, F. (1990) *J. Mol. Biol.* **212,** 513–539
20. Lu, G., Stec, B., Giroux, E. L., and Kantrowitz, E. R. (1996) *Protein Sci.* **5,** 2333–2342
21. Zhang, Y., Liang, J.-Y., Huang, S., and Lipscomb, W. N. (1994) *J. Mol. Biol.* **244,** 609–624
22. Gibbons, I., and Schachman, H. K. (1976) *Biochemistry* **15,** 52–60
23. Gibbons, I., Ritchey, J. M., and Schachman, H. K. (1976) *Biochemistry* **15,** 1324–1330
24. Yang, Y. R., and Schachman, H. K. (1980) *Proc. Natl. Acad. Sci. U. S. A.* **77,** 5187–5191
25. Lahue, R. S., and Schachman, H. K. (1986) *J. Biol. Chem.* **261,** 3079–3084
26. Fushinobu, S., Kamata, K., Iwata, S., Sakai, H., Ohta, T., and Matsuzawa, H. J. (1996) *J. Biol. Chem.* **271,** 25611–25616
27. Fushinobu, S., Ohta, T., and Matsuzawa, H. (1998) *J. Biol. Chem.* **273,** 2971–2976
28. Nelson, S. W., Honzatko, R. B., and Fromm, H. J. (2001) *FEBS Lett.* **492,** 254–258
29. Kelley-Loughnane, N., and Kantrowitz, E. R. (2001) *Proteins* **44,** 255–261
30. Laemmli, U. K. (1970) *Nature* **227,** 680–685
31. Bradford, M. M. (1976) *Anal. Biochem.* **72,** 248–252
32. Cornish-Bowden, A. J., and Koshland, D. E., Jr. (1971) *J. Biol. Chem.* **246,** 3092–3102
33. Lui, F., and Fromm, H. J. (1990) *J. Biol. Chem.* **265,** 7401–7406
34. Leatherbarrow, R. J. (1987) *ENZFITTER: A Non-Linear Regression Data Analysis Program for the IBM PC*, pp. 13–75, Elsevier Science Publishers, Amsterdam
35. Chiadmi, M., Navaza, A., Miginiac-Maslow, M., Jacquot, J. P., and Cherfils, J. (1999) *EMBO J.* **18,** 6809–6815
36. Roitel, O., Sergienko, E., and Branlant, G. (1999) *Biochemistry* **38,** 16084–16091
37. Shyur, L.-F., Aleshin, A. E., Honzatko, R. B., and Fromm, H. J. (1996) *J. Biol. Chem.* **271,** 3005–3010
38. Shyur, L.-F., Aleshin, A. E., and Fromm, H. J. (1996) *Biochemistry* **35,** 7492–7498
39. Shyur, L.-F., Aleshin, A. E., Honzatko, R. B., and Fromm, H. J. (1996) *J. Biol. Chem.* **271,** 33301–33307
40. Lu, G., Giroux, E. L., and Kantrowitz, E. R. (1997) *J. Biol. Chem.* **297,** 5076–5084
41. Shyur, L.-F., Poland, B. W., Honzatko, R. B., and Fromm, H. J. (1997) *J. Biol. Chem.* **271,** 26295–26299
42. Carcamo, J. G., Yanez, A. J., Ludwig, H. C., Leon, O., Pinto, R. O., Reyes, A. M., and Slebe, J. C. (2000) *Eur. J. Biochem.* **267,** 2242–2251
43. Kurbanov, F. T., Choe, J.-Y., Honzatko, R. B., and Fromm, H. J. (1998) *J. Biol. Chem.* **273,** 17511–17516
44. Kelley, N., Giroux, E. L., Lu, G., and Kantrowitz, E. R. (1996) *Biochem. Biophys. Res. Commun.* **219,** 848–852
45. Nelson, S. W., Choe, J.-Y., Honzatko, R. B., and Fromm, H. J. (2000) *J. Biol. Chem.* **275,** 29986–29992
46. McGrane, M. M., El-Maghrabi, M. R., and Pilkis, S. J. (1983) *J. Biol. Chem.* **258,** 10445–10454
47. Iversen, L. F., Brzozowski, M., Hastrup, S., Hubbard, R., Kastrup, J. S., Larsen, I. K., Nærun, L., Nørskov-Lauridsen, L., Rasmussen, P. B., Thim, L., Wiberg, F. C., and Lundgren, K. (1997) *Protein Sci.* **6,** 971–982
48. Ackers, G. K., Doyle, M. L., Myers, D., and Daugherty, M. A. (1992) *Science* **255,** 54–63

Hybrid Tetramers of Porcine Liver Fructose-1,6-bisphosphatase Reveal Multiple Pathways of Allosteric Inhibition

Scott W. Nelson, Richard B. Honzatko and Herbert J. Fromm

Access the most updated version of this article at doi: 10.1074/jbc.M112304200

Alerts:
- When this article is cited
- When a correction for this article is posted

Click here to choose from all of JBC's e-mail alerts

This article cites 47 references, 18 of which can be accessed free at
http://www.jbc.org/content/277/18/15539.full.html#ref-list-1